An investigation into the effects of geometric scaling and pore structure on drug dose and release of 3D printed solid dosage forms

Thomas Mcdonagh[a], Peter Belton[b], Sheng Qi[a]*

[a]School of Pharmacy, University of East Anglia, Norwich, UK

[b]School of Chemistry, University of East Anglia, Norwich, UK

* Corresponding author. E-mail: *sheng.qi@uea.ac.uk*

Abstract

A range of 3D printing methods have been investigated intensively in the literature for manufacturing personalised solid dosage forms, with infill density commonly used to control release rates. However, there is limited mechanistic understanding of the impacts of infill adjustments on *in vitro* performance when printing tablets of constant dose. In this study, the effects and interplay of infill pattern and tablet geometry scaling on dose and drug release performance were investigated. Paracetamol (PAC) was used as a model drug. An immediate release erodible system (Eudragit E PO) and an erodible swellable system (Soluplus) were prepared via wet granulation into granules and printed using Arburg Plastic Freeforming (APF). Both binary formulations, despite not FDM printable, were successfully APF printed and exhibited good reproducibility compared to pharmacopoeia specification. The physical form of the drug and its integrity following granulation and printing was assessed using DSC, PXRD and ATR-FTIR. Two infill patterns (SM1 and SM2) were employed to print tablets with equal porosity, but different pore size, structure and surface area to volume ratio (SA/V). Geometry scaling (tablet height and diameter) of Eudragit-PAC tablets was not found to significantly influence the release rate of the tablets with 30 to 70% infill density. When increased to 90% infill density, geometric scaling was found to have a significant effect on release rate with the constant diameter tablet releasing faster than the constant height tablet. Soluplus-PAC tablets printed using different infill patterns demonstrated similar release profiles, due to swelling. Geometric parameters were found to significantly influence release profiles for tablets printed at certain infill densities giving new insight into how software parameters can be used to tune drug release.

Key words: Arburg Plastic Freeforming (APF), thermal droplet deposition 3D printing, infill density, constant dose, shape fidelity, controlled drug release.

Introduction

3D printing (3DP), as a group of additive manufacturing (AM) technologies, is rapidly emerging as a key tool for manufacturing personalised treatments. Already used in the manufacture of individualised prosthetics and some medical devices, there has been great research interest for potential applications in pharmaceutics. Unlike traditional manufacturing techniques, AM can be utilised to print unique geometries with different release and dosage properties to suit individual patient needs without changing infrastructure and raw materials [1, 2]. For 3D printing personalised medicine, both the volume of material deposited, and tablet geometry can be tuned to meet patient specific drug dose and release requirements, respectively (**Figure 1**). When considering tuning drug dosage of 3DP solid dosage forms, there are two feasible methods: controlling the size (mass) of the tablet by changing the volume of material deposited or altering the drug loading of the formulation. Altering tablet size is by far the most practical method because it can be achieved in software so no adjustment to the feedstock is required. Using this method, a 'universal feedstock' can be developed for each drug to be used for patients with different dose requirements.

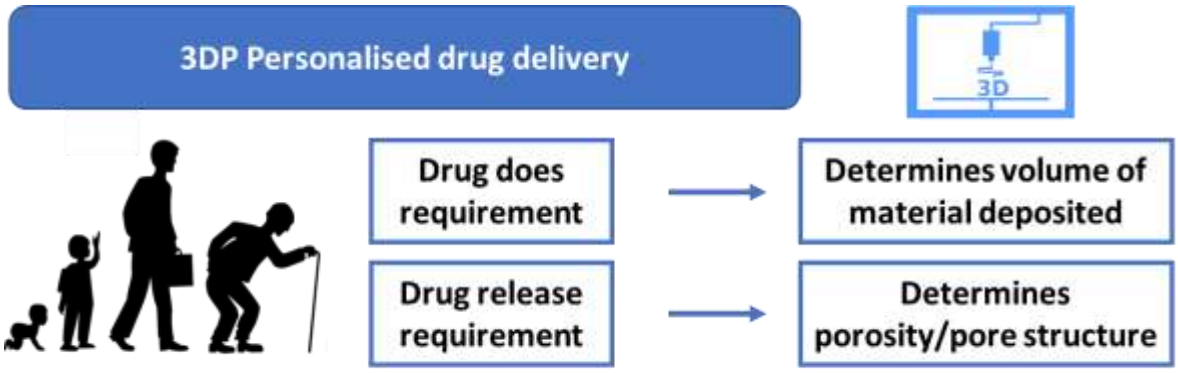

Figure 1. Method of geometry controlled 3DP personalised drug delivery

Controlling drug release rate using 3DP can be achieved by manipulating a wide range of parameters which can be described as formulation related or geometry related [3]. In this study

we focus on geometry mediated drug release because tuning can be achieved in software, independent of the formulation used, enabling the printing of solid dosage forms with a wide range of release profiles from a single feedstock [4, 5]. Both tablet outer geometry (diameter and height) and inner geometry (the voids formed by the interfilament spacing which we term pores) can be tuned. The effects of tablet outer geometry scaling on release performance have been well studied for solid dosage forms with release rate considered to be largely dependent on surface area to volume ratio (SA/V) and aspect ratio (height to diameter ratio) [6-8]. However, to our knowledge the effect of geometric scaling on porous 3DP dosage forms have not been explored which forms the first area of interest of this study. For inner geometry literature data suggests that tablet pore structure mediates drug release rates by changing tablet SA/V and pore fluid dynamics [9, 10]. In 3DP, the degree of porosity of a print, which are the voids created as a results of printing using less than 100% infill, is controlled by changing a slicing software parameter, infill density which controls how closely printpaths are deposited next to each other during printing [5, 11, 12]. Additionally, different infill patterns, such as rectilinear, cubic and hexagonal, can be used to produce different pore structures within the dosage form. Both infill density and infill pattern can be varied to produce solid dosage forms with significantly different SA/V ratios and pore structures to mediate release performance. For pharmaceutical applications to date, the effects of infill pattern on the performance of printed pharmaceuticals have not been fully understood. This is the second area of interest of this study.

The aim of this study is to investigate how both drug dose and release requirements can be met using simple software/slicing design changes. Tablet scaling can be used to maintain dose whilst varying infill density. To enrich understanding, we investigated printing constant dose tablets with infill densities ranging from 30% - 90% and explored the effects of tablet height

and diameter scaling on drug release. A second formulation was used to print porous tablets from 30% - 90% infill density using two different infill patterns to generate structures with significantly different pore structure in terms of pore size and SA/V. The first infill pattern (SM1) was used to print tablets with a small interconnected porous structure and a second infill pattern (SM2) was used to print tablets with larger unconnected pores. Eudragit® E PO, an erodible polymer, soluble at low gastric pH suitable for immediate release applications was used to study the effects of outer geometry scaling and Soluplus an erodible swellable polymer suitable for sustained release applications was used to study the effects of infill pattern. Paracetamol was used as a model drug. Tablets were printed using Arburg plastic freeforming (APF), a novel direct granule thermal deposition 3DP technique which has shown promise in a previous study for printing materials not suitable for fused deposition modelling (FDM) printing [4]. Both Eudragit E and Soluplus cannot be printed by FDM without additives, such as plasticisers due to their high melt viscosity and brittleness [13, 14]. The outcome of the study not only demonstrated the capacity of APF for direct printing of pharmaceutical polymers without the need of additives, such as plasticisers, but more importantly outlined the clear correlations between outer- (i.e., tablet dimensions) and inner-structures (pore structure) of the dosage form on drug release performance.

Materials and Methods

Materials

Eudragit® E PO was kindly donated by Evonik (Evonik Industries, Germany), Soluplus® was kindly donated by BASF (Ludwigshafen, Germany) and the model drug, paracetamol (PAC), was purchased from Molekula (Molekula Ltd, United Kingdom).

Feed material (granules) preparation

Eudragit EPO and Soluplus were used as the polymeric matrix excipients to prepare the two paracetamol loaded formulations. In this study, these two formulations are named as Eudragit-PAC (as a model of erodible tablets) and Soluplus-PAC (as a model of swellable and erodible tablets). For both formulations a drug: polymer ratio of 4:10 (w/w) was used giving a drug loading of 28.6% (w/w). All materials were accurately weighed and premixed in a Kenwood food mixer with flat beater attachment for 5 minutes. To agglomerate the powder into granules 50% v/w Milli-Q water was added, and the formulations were further mixed for 15 minutes. Wet granules were subsequently removed from the food mixer, spread thinly over baking trays and placed in an oven set to 40°C overnight. Once dried, granules would fall apart on light handling. An 850μm and 2mm sieve were used to collect granules of more uniform size distribution. Following preliminary granule characterisations from a previous study [4] granules between 850μm and 2mm were selected for printing.

APF printing of tablets

An Arburg Plastic Freeformer (APF) equipped with 2 piezo actuated thermal extrusion heads (200μm nozzle diameter) was used for printing the drug loaded tablets. Digital CAD files for the 3D geometries were generated in SOLIDWORK and exported to Arburgs proprietary slicing software (Freeformer software V2.2, Arburg, Germany) as an STL file. Tablets were printed onto a vacuum held Teflon build plate. Cylindrical tablets were printed with default dimensions of 10 mm diameter, and 4mm height. These dimensions were varied when studying the effects of outer geometry scaling (See section on constant dose tablet printing). Printing conditions are shown in **Table 1**.

Table 1. APF printing conditions for Eudragit-PAC and Soluplus-PAC tablets

Feed material	Nozzle diameter (µm)	Temperatures (°C)			Build chamber temperature (°C)	Discharge (%)	Printing Pressure (bar)	Aspect Ratio (AR)	Layer height (mm)
		Zone 1*	Zone 2	Discharge nozzle					
Eudragit-PAC	200	115	125	140	45	120	500-600	1.75	0.2
Soluplus-PAC	200	115	130	150	50	80	400-500	1.5	0.2

Note*: Zone 1 is close to the feeding hooper and zone 2 is close to the discharge nozzle.

Modelling printed tablets

SOLIDWORKs CAD models were used to investigate the printed tablet pore structure and surface area. The theoretical design of tablets is shown in **Figure 2a**. Whilst APF is a droplet-based printing technique, discharged drops were observed to merge into elliptical cylinders, known as printpaths (**Figure 2b**) which formed the basis of the CAD model. Theoretical printpath geometry was calculated using a volume conservation approach considering the volume of material deposited in each user defined drop/voxel. For example, for Soluplus-PAC tablets, a layer height of 0.2mm and an aspect ratio of 1.5 was used defining a voxel geometry of 0.3 x 0.3 x 0.2mm. This cuboidal voxel geometry is only realised when printing at 100% infill density. At lower infill densities printpaths maintain their elliptical geometry. By equating the voxel volume to that of an elliptical cylinder using the known aspect ratio of the material we approximated the true printpath dimensions. For Soluplus-PAC tablets, this gave an equivalent drop height of 226 µm and an equivalent droplet width of 339 µm. These values are significantly higher than the voxel dimensions as expected and corresponded well with the SEM images of porous prints (**Figure 2b** and **c**). These dimensions were used to create a refined CAD model that better modelled the merging between droplets and the level of overlap seen at filament intersections and between layers.

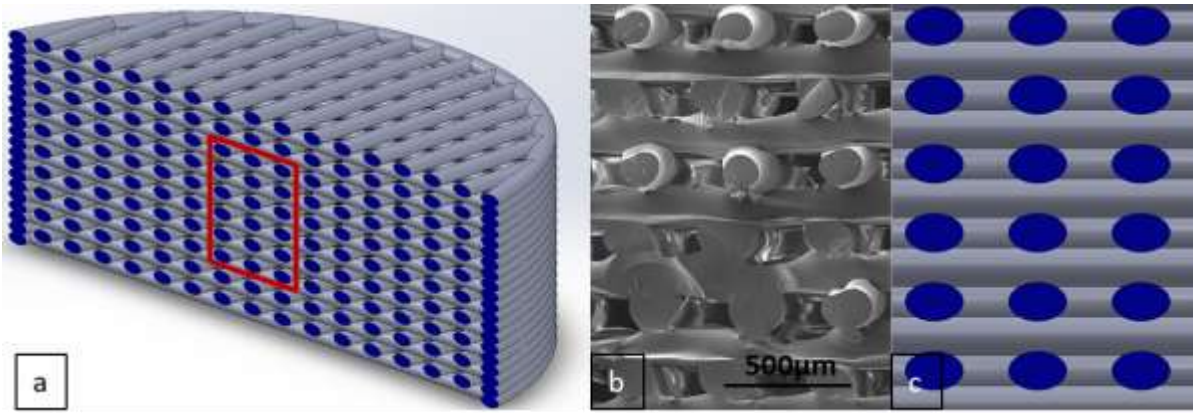

Figure 2. Cross-section of theoretical CAD model of Soluplus-PAC APF printed tablet at 50% infill density (a); SEM image of the cross section of Soluplus-PAC tablets (b) compared with close-view of the theoretical model (c).

Altering infill patterns by changing slicing methods

Two infill patterns were used to produce different pore geometries to explore how pore structure effects drug release performance for our model swellable, erodible system, Soluplus-PAC. The two infill patterns have been denoted slicing method 1 (SM1) and slicing method 2 (SM2). SM1 is the default infill pattern used by the proprietary APF freeformer software and most other 3D printing software often caller rectilinear and produces a rectangular interconnected pore structure shown in **Figure 3a**. SM1 was used for all Eudragit-PAC prints. For SM1 spacing between adjacent filaments is calculated based on the aspect ratio of the material drop (**Eq. 1**), layer thickness and the desired infill-density.

$$Spacing\ between\ adjacent\ rows = \frac{layer\ height \times Aspect\ ratio}{Infill\ density\ (\%)} \qquad \textbf{Eq.1}$$

Slicing method 2 (SM2) was used to create structures with larger but disconnected pores to explore effects of SA/V ratio and fluid dynamics whilst maintaining consistent drug dose between designs. This infill pattern is commonly called grid and is shown in **Figure 3b**. Spacing between adjacent rows is twice that of SM1.

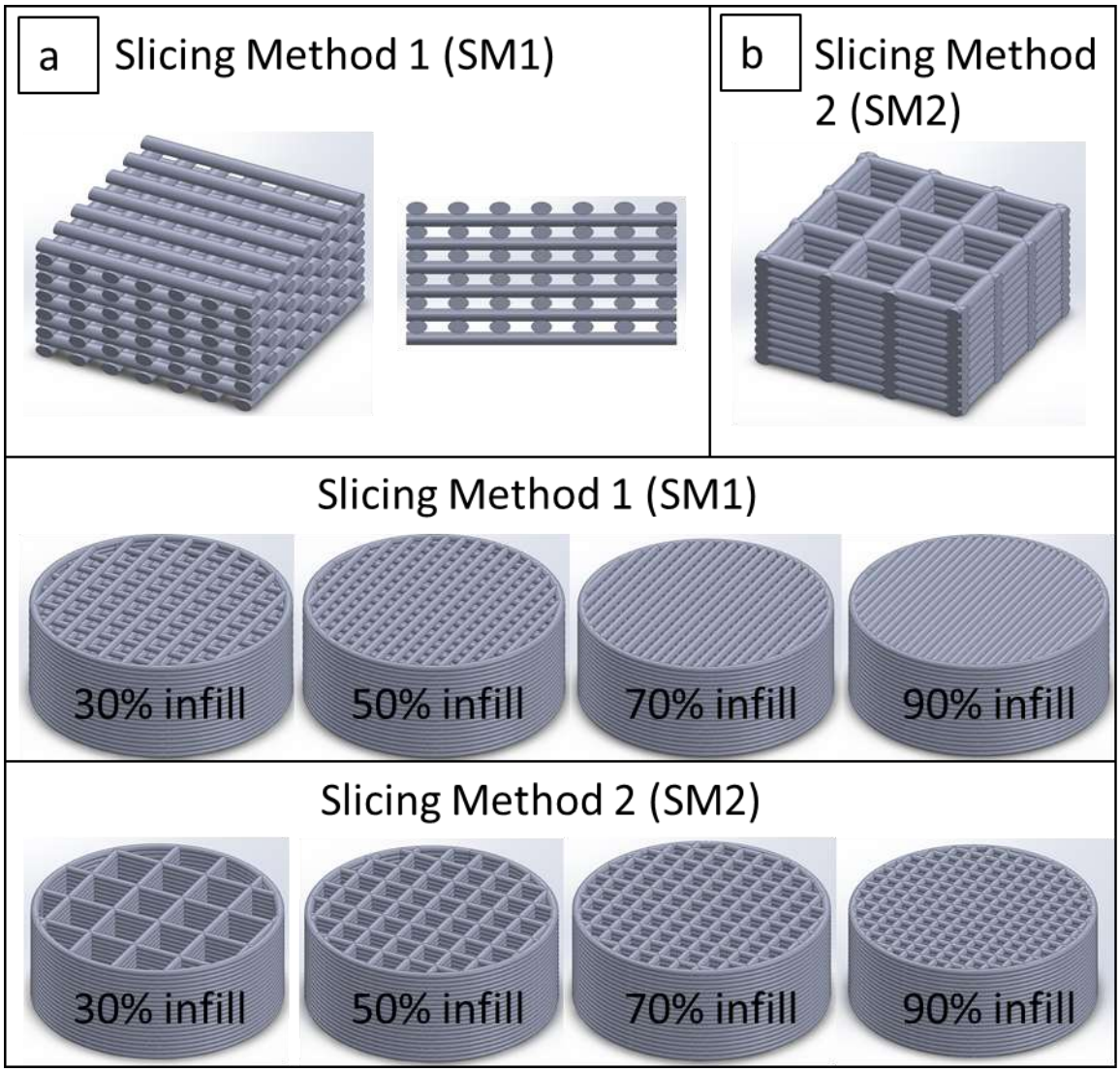

Figure 3. Top roll – the comparison of the CAD file of 50% infill cube generated using (a) slicing method 1 (SM1) and the (b) slicing method 2 (SM2); middle roll- modelled Soluplus-PAC tablets using SM1; and bottom roll- modelled Soluplus-PAC tablets using SM2

Constant dose tablet printing

The targeted dimensions of the Eudragit-PAC printed tablets with constant dose but varying infill density were calculated using an experimental approach. An initial batch of Eudragit-PAC tablets with dimensions 4mm in height, 10mm in diameter were printed at infill densities from 30-90%. The mass of prints at each infill density (M_i) was recorded enabling calculation of respective tablet density (D_i) using **Eq. 2:**

$$D_i = \frac{M_i}{\pi r^2 h} \qquad \textbf{Eq. 2}$$

Assuming cylindrical symmetry with radius, r, and height, h.

If target mass, M_t, is to be kept constant for different infills the required macro tablet volume must be adjusted. Required tablet volume, V_i, can be calculated using **Eq. 3**.

$$V_i = \frac{M_t}{D_i} \qquad \textbf{Eq. 3}$$

Corresponding tablet height and diameter dimensions can subsequently be calculated by fixing either variable. At fixed height, h_f, tablet diameter is given by **Eq. 4** and at fixed diameter, d_f, tablet height is given by **Eq. 5**.

$$d_i = \frac{2V_i}{\sqrt{h_f \pi}} \qquad \textbf{Eq. 4}$$

$$h_i = \frac{V_i}{\pi(\frac{d_f}{2})^2} \qquad \textbf{Eq. 5}$$

Using this method target dimensions for constant dose Eudragit-PAC tablets at different infill densities were established (**Table 2**). Tablet diameter was fixed at 10mm for constant diameter tablets and tablet height was fixed at 4mm for constant height tablets.

Table 2. Target tablet dimension for *constant dose* Eudragit-PAC tablets

Tablet infill density (%)	**Constant diameter target dimensions**		**Constant height target dimensions**	
	Diameter (mm)	**Height (mm)**	**Diameter (mm)**	**Height (mm)**
30	10	6.96	13.19	4
40	10	5.69	11.92	4
50	10	4.81	10.96	4
60	10	4.17	10.2	4
70	10	3.67	9.58	4
80	10	3.29	9.06	4
90	10	2.97	8.62	4

*Target heights were rounded to the nearest multiple of 0.2 (the layer height) during printing.

Differential Scanning Calorimetry (DSC)

DSC was conducted using a DSC2500 differential scanning calorimeter (TA Instruments, Newcastle, United States) to detect glass transition temperatures (T_g) and melting peaks for the different formulations. Raw materials, physical blends, granules and printed samples were characterised using a heat ramp with a temperature range of 0 °C to 200°C at 10 °C/min with 1 minute isothermal at 0 °C. Sample weights were 2–5 mg contained in an aluminium standard TA crimped pans and lids (TA Instruments, Newcastle, USA). All tests were done in triplicates.

Attenuated total reflectance Fourier transform infrared spectroscopy (ATR-FTIR)

ATR-FTIR measurements were conducted using a Vertex 70 FTIR spectrometer (Bruker Optics Ltd., United Kingdom), equipped with a Golden Gate, heat-enabled Attenuated Total Reflectance (ATR) accessory (Specac Ltd., Orpington, United Kingdom) fitted with a diamond internal reflection element. ATR-FTIR spectra were acquired in absorbance mode, using a resolution of 4 cm^{-1}, 128 scans for each sample, within the range of wavenumbers from 4000 cm^{-1} to 600 cm^{-1}. Spectra analysis was conducted using OPUS version 7.8 (Bruker Optics Ltd., United Kingdom). All measurements were done in triplicate.

Powder X-ray diffraction (PXRD)

A SmartLab SE X-ray diffractometer (Rigaku, Tokyo, Japan) with monochromatic CuKα radiation (wavelength = 1.54056 Å) was used to measure the raw materials, the granules and the APF printed tablets. The extrudates and the printed tablets were briefly grinded to powder form prior to their measurements. A scanning range of $5° < 2\theta < 60°$, with a step width of 0.02° and a scan speed of 4°/minute was used to conduct all measurements.

Scanning Electron Microscopy (SEM)

A GeminiSEM300 SEM (Zeiss, Oberkochen, Germany) was used to study the size and surface morphology of printed tablets. All samples were attached to SEM stubs using double adhesive tape and then coated with gold using a Polaron SC7640 sputter gold coater (Quorum Technologies, Lauphton, UK) prior to imaging.

Drug content measurement

Accurately weighed drug loaded printed material was dissolved in a beaker containing 150 ml of 0.1 M pH 1.2 HCl (n = 6) for Eudragit-Pac samples or 6.8pH PBS for Soluplus-Pac samples. The medium was stirred using a magnetic stirrer at room temperature until complete dissolution of all material. From this solution, 1 ml samples were withdrawn and filtered through a membrane filter with 0.45 µm pore size (Minisart NML single use syringe, Sartorius, UK). The drug concentrations of the samples were analysed using a UV–VIS spectrophotometer (Perkin-Elmer lambda 35, USA) at 243 nm using a UV cell with 1 cm pathlength. The drug content measurements were carried out in triplicate.

***In vitro* drug release studies**

The in vitro drug release profiles were measured in dissolution testing apparatus (Caleva 8ST, Germany) using the basket method (USP apparatus 1). A basket rotation speed of 100 rpm at 37 ± 0.5 °C were used for all measurements. For Eudragit-PAC tablets, 900 ml of pH 1.2 HCl were used as the dissolution media and the dissolution tests were carried out for 120 minutes. For Soluplus-PAC tablets, 900 ml pH 6.8 phosphate buffer was used the dissolution media and all tests were carried out for 22 hours. 5ml dissolution samples were withdrawn at pre-determined time intervals. The samples were directly filtered through a membrane filter with 0.45 µm pore size (Minisart NML single use syringe, Sartorius, UK). The samples were

analysed using a UV–VIS spectrophotometer (Perkin-Elmer lambda 35, USA) at 243 nm for paracetamol detection and quantification. All dissolution tests were performed under sink conditions. All drug release studies were conducted in triplicate.

In vitro drug release data analysis

Mean Dissolution time (MDT) was used to compare the release rates of the different designs. MDT is a model independent parameter that allows the direct comparison of drug release rates of dosage forms [5, 15-17]. The MDT is the time at which 50% of the drug is dissolved from its solid state under dissolution conditions (**Eq. 6**). Such mathematical analyses enable statistical comparisons between the various formulations.

$$MDT = \frac{\sum_{j=1}^{n} t_{j*} \ \Delta M_{j*}}{\sum_{j=1}^{n} \Delta M_{j*}} \qquad \textbf{Eq. 6}$$

where j is the sample number, n is the number of dissolution sample times, t_{j*} is the time at a midpoint between t_j and t_{j-1} and ΔM_{j*} is the additional amount of drug dissolved between t_j and t_{j-1}.

Tablet dissolution images

Images were captured of the tablets during dissolution under the same conditions as the in vitro drug release study to help understand the mechanisms of drug release. To capture the images, the dissolution was paused at certain time intervals and baskets containing the tablets were raised out of the dissolution media and drained. The basket cap was then removed, and a top-down image was taken of the tablet. Whilst care was taken to minimise time whilst the dissolution was paused it was impossible to avoid some dissolution that occurs during the taking of the image.

Results and discussion

Effects of pore structure on theoretical surface area to volume (SA/V) ratio

Drug release rate from water soluble and swellable polymers is mainly governed by the relative contribution of two mechanisms, drug diffusion and matrix dissolution/erosion [18]. These mechanisms are known to be highly influenced by the SA/V ratio of the dosage form [5, 8, 19, 20]. Increased SA/V increases the relative rate of erosion and swelling increasing the rate at which drug dissolves in the dissolution media [21] [22, 23]. Whilst SA/V ratios are easy to calculate for non-porous solid geometries, for highly porous printed lattice geometries, surface area is highly dependent of the amount of merging that occurs between adjacent filaments/drops and between layers.

When considering the effect of infill density on SA/V, the trend of decreasing infill density (increasing porosity) increasing the SA/V ratio of the tablet which results in increased drug release rates is well accepted. However, the understanding of how infill density changes SA/V ratio is rarely described. Lattice structures, such as the printed tablets described in this study (**Figure 4a**), can be thought of as stacks of cylinders that are arranged as a woodpile structure. If no overlap between these cylindrical subunits is considered, the SA/V ratio of any structure consisting of these will be the same no matter the spacing or arrangement. In reality, during printing, there is merging at the interface of these cylinders (which are known in printing as printpaths), which reduces the exposed surface area. It is therefore the magnitude of overlapping and the quantity of instances of overlapping that mediates print SA/V. Printing parameters, such as temperature, can be used to control the magnitude of overlap, with higher temperatures causing increased material melting thus a higher degree of merging [24]. However, this is rarely used for mediating surface area as temperature changes will drastically affect print quality. Infill density is the main parameter which is used to control SA/V ratio and

does so by controlling the quantity and spacing of adjacent printpaths. For higher infill densities there is an increased quantity of printpaths in the infill resulting in more instances of overlapping. This overlap is generally in the z-direction, as illustrated in **Figure 4b**. However, there is a critical infill density (I_c) that when surpassed results in overlap of the printpaths in the x and y directions as well as the z direction. When printing at infill densities above I_c, inter-filament spacing is less than droplet width (DW) resulting in porous channels that are no longer open and interconnected. This dramatically reduces the exposed surface area. When using SM1, the theoretical I_c for both formulations is 89%.

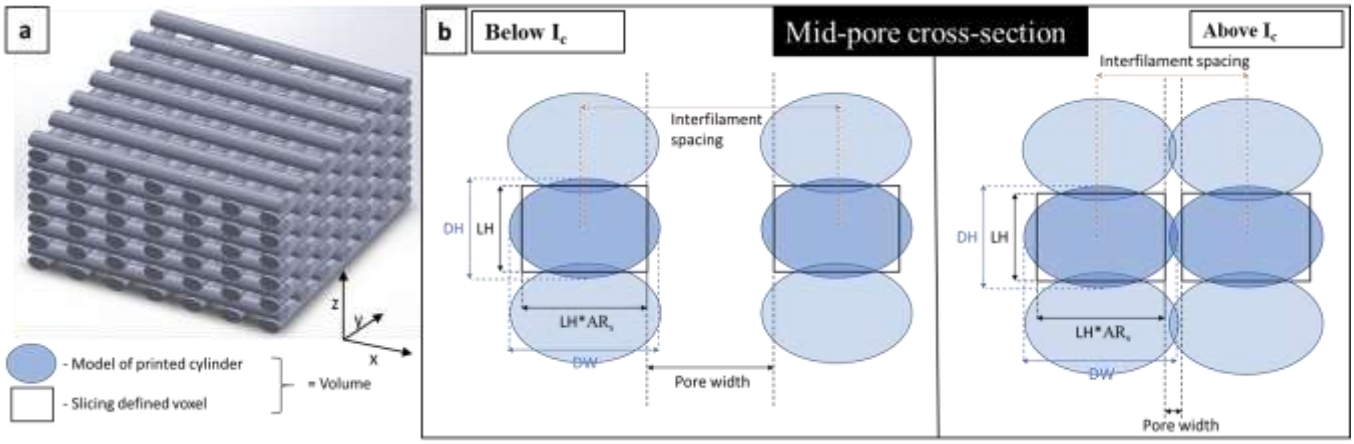

Figure 4. (a) 3D model of APF printed lattice structure using slicing method 1 (SM1). (b) 2D depiction of theoretical printed mid-pore cross-section at infill densities below and above I_c. LH is the slicer defined layer height. AR_s is the slicer aspect ratio. DW and DH are the actual printpath dimensions (DW = droplet width, DH = droplet height).

CAD models were used to model the overlap between printpaths to better understand the SA/V for the two different infill patterns used for printing (shown in **Table 3 and 4**). Slicing method 1 (SM1) is the default infill pattern used by APF printer and creates an interconnected porous lattice. Slicing method 2 (SM2) deposits approximately the same amount of material as SM1 but creates a structure with larger unconnected pores as described in the methods section. Irrespective of the infill pattern used, increased infill density resulted in decreased SA/V ratio.

As discussed, this is due to increased instances of printpath overlap at the higher infill densities. Interestingly, there is a significant difference in the SA/V ratios between the two infill patterns at each infill density, despite being of approximately equal volume (**Table 3**). SA/V ratios calculated from the structures generated using SM1 are consistently 45 -55% higher than the ones generated by SM2. This is because the resultant structures generated using SM2 have increased instances of overlap. Pore width (as defined in **Figure 3b**) is much greater for SM2, varying from 2.43 times greater at 30% infill to 11.12 times greater at 90% infill.

Table 3. Theoretical tablet surface area to volume ratio based on CAD models of printed Soluplus-PAC tablets using SM1 and SM2 (tablet dimensions: 10 mm diameter, 4 mm height)

Design	***Pore width (mm)***	***SA (mm^2)***	***V (mm^3)***	***SA/V***
SM1 (30% infill)	0.7	1457.16	120.32	12.11
SM2 (30% infill)	1.7	1017.42	121.78	8.35
SM1 (50% infill)	0.3	2072.21	177.79	11.66
SM2 (50% infill)	0.9	1351.56	176.56	7.65
SM1 (70% infill)	0.129	2599.55	234.96	11.06
SM2 (70% infill)	0.557	1592.77	233.96	6.81
SM1 (90% infill)	0.033	2703.95	291.24	9.28
SM2 (90% infill)	0.367	1741.93	289.84	6.01
Solid (100% infill)	0	282.74	314.16	0.90

For Eudragit-PAC tablets, the infill pattern (SM1) was kept the same between designs whilst changing the geometric scaling by either varying the tablet diameter or height. This allowed tablet volume and subsequently the drug dose to be kept fairly consistent, indicated by the

similar theoretical volume calculations in **Table 4**. Tablet dimension scaling did not lead to significant change in calculated SA/V ratios of the tablets (**Table 4**).

Table 4. Theoretical tablet surface area to volume ratio based on CAD models of printed Eudragit-PAC constant dose tablets using SM1 (the dimensions data are shown in ***Table 2***)

Design	***Pore width (mm)***	***SA (mm^2)***	***V (mm^3)***	***SA/V***
30% infill CD	0.82	2226.71	194.10	11.47
30% infill CH	0.82	2162.81	181.83	11.89
50% infill CD	0.35	2153.11	189.20	11.38
50% infill CH	0.35	2173.43	189.73	11.46
70% infill CD	0.15	2043.28	184.97	11.05
70% infill CH	0.15	2084.21	190.67	10.93
90% infill CH	0.039	1927.83	207.88	9.27
90% infill CD	0.039	1869.82	204.84	9.13

Physicochemical characterisation of APF printed tablets

The morphological differences between the APF printed discharged filaments of Eudragit-PAC and Soluplus-PAC are apparent, as shown in **Figure 5**. Paracetamol crystals were clearly visible on the surface of the Eudragit-PAC filaments whereas for comparison the Soluplus-PAC filaments surface showed no visible signs of crystallinity. With the same drug loading, this indicates PAC recrystallised after printing. This may be caused by the difference in drug-polymer miscibility between formulations and was investigated further using a range of other characterisation methods [25].

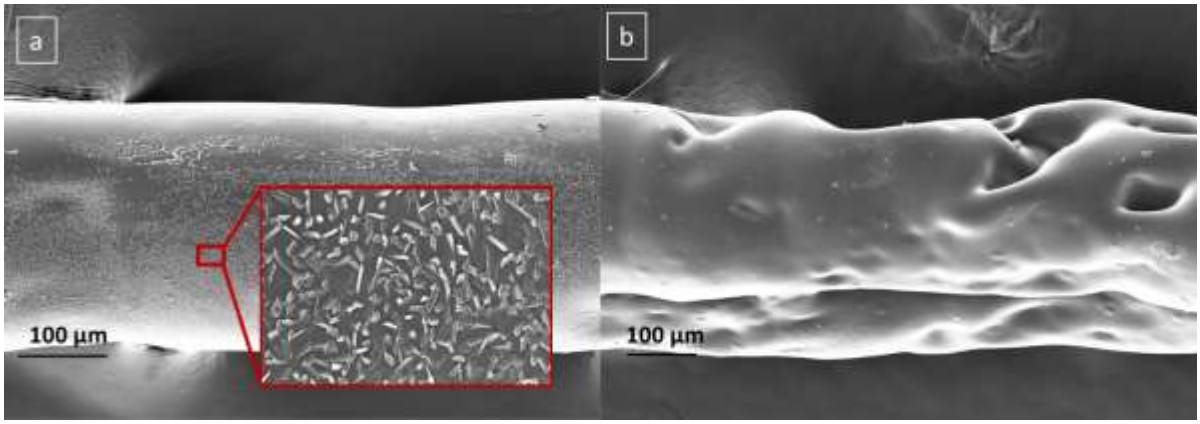

Figure 5. APF discharge of (a) Eudragit-PAC formulation with paracetamol crystals visible on surface (insert); (b) Soluplus-PAC formulation

PXRD data, shown in **Figures 6a** and **6b,** suggests that both formulations are mostly in crystalline form in the granules which is expected at the moderate drug loading used in this study (28.6% w/w). For the Eudragit-PAC printed sample (**Figure 6a),** the PXRD pattern remain largely unchanged from the pattern of the granules, with some minimal peak reduction at 12.1 and 13.8, 23.4, 24.3 and 26.5 ° 2θ, indicating the recrystallisation of PAC in the APF printed Eudragit-PAC tablets. Conversely, the PXRD pattern of printed Soluplus-PAC is an amorphous halo with no visible peaks, indicating the formation of an amorphous solid dispersion. This data is in good agreement with the SEM observations.

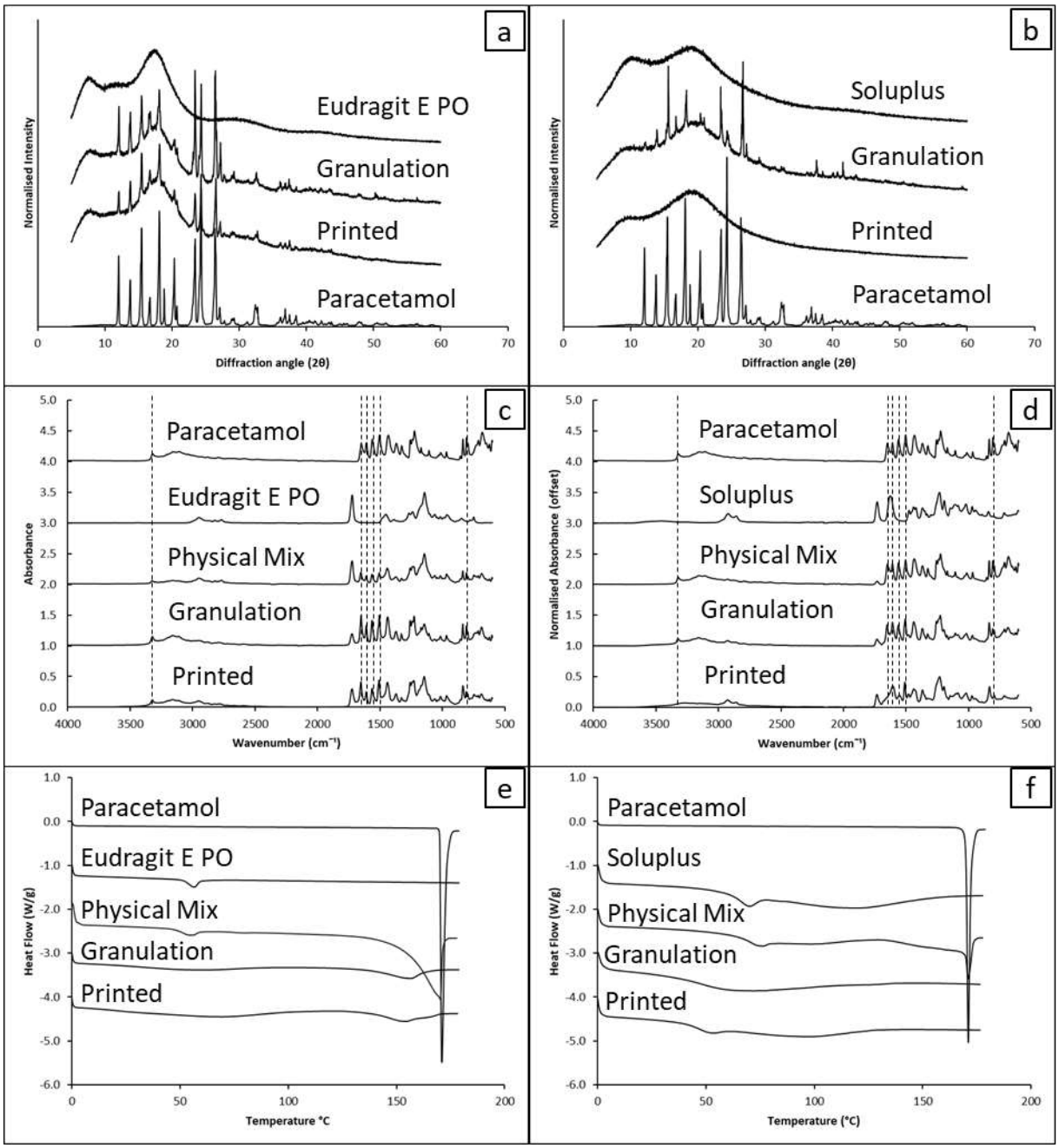

Figure 6. (a) the PXRD pattern of Eudragit-PAC; (b) the PXRD pattern of Soluplus-PAC (c) ATR-FTIR spectra of the raw excipients, physical mixture (PM), granules and APF printed for Eudragit-PAC tablets; (d) ATR-FTIR spectra of the raw excipients, physical mixture (PM), granules and APF printed for Soluplus-PAC tablets; (e) DSC thermogram illustrating different thermal events for Eudragit-PAC formulation (Heat flow values for crystalline paracetamol scaled by 0.5); (f) DSC thermogram illustrating different thermal events for Soluplus-PAC formulation (Heat flow values for crystalline paracetamol scaled by 0.5).

ATR-FTIR data is shown in **Figures 6c** and **6d**. Characteristic vibrational peaks for N-H and OH stretching are seen at 3321, and 3180 – 3035 cm^{-1}, respectively. Additional signature peaks

of crystalline PAC in the fingerprint region at 1651, 1608, 1562, 1506 and 808 cm^{-1} have been highlighted. No peak shifting was seen when comparing the spectra of Eudragit-PAC physical mix to the printed sample, indicating no strong interaction between drug and polymer and the presence of a large percentage of crystalline drug. The lack of drug-polymer interaction may contribute to the poor drug-polymer miscibility, thus rapid drug recrystallisation after printing [25]. This was not the case for APF printed Soluplus-PAC tablets. In the Soluplus-PAC spectra, the N-H peak at 3321 cm^{-1} becomes very broad, which is characteristic of amorphous paracetamol, similarly peaks in the fingerprint region also broaden as would be expected for the amorphous form [26], [27].

The DSC results of the raw materials, physical mixes and printed tablets are shown in **Figure 6e** and **6f**. The melting peak of crystalline paracetamol occurred at 170 °C and a glass transition temperature (T_g) of 56.6 °C and 70.2 °C was identified for Eudragit E PO and Soluplus, respectively, agreeing with reported literature data [28-30]. The DSC result of the physical mix of Edugrait-PAC shows depressed onset of crystalline PAC melting. For Eudragit-PAC granules and printed tablets, further depressed melting peaks with reduced enthalpy values of the crystalline drug melting were observed in comparison to crystalline PAC. The melting point depression of PAC is likely caused by the presence of Eudragit in the course of the DSC heating. The presence of melting confirms the recrystallisation of PAC after printing, aggreging with SEM, PXRD and ATR-FTIR data. The measured T_g of Eudragit reduced significantly to 29 °C and 23 °C after granulation and printing, due to the plasticisation of molecularly dispersed paracetamol. The lower T_g of the printed Eudragit-PAC than the granules indicates more amorphous PAC was present after printing. The absence of a crystalline PAC melting in the DSC results of the printed Soluplus-PAC tablets indicates the printed formulations being amorphous solid dispersion which is in agreement with other characterisation data. The

characterisation data suggests that despite equal drug loading between the two formulations, Soluplus has greater miscibility with PAC than Eudragit.

Key quality attributes of APF printed tablets

Both granule formulations were found to be suitable for APF 3D printing directly without the need for additives, such as plasticisers. Printed tablets showed good adhesion between layers. The levels of printing defects of the tablets are more visible in the tablets printed with low infill density (**Figure 7**).

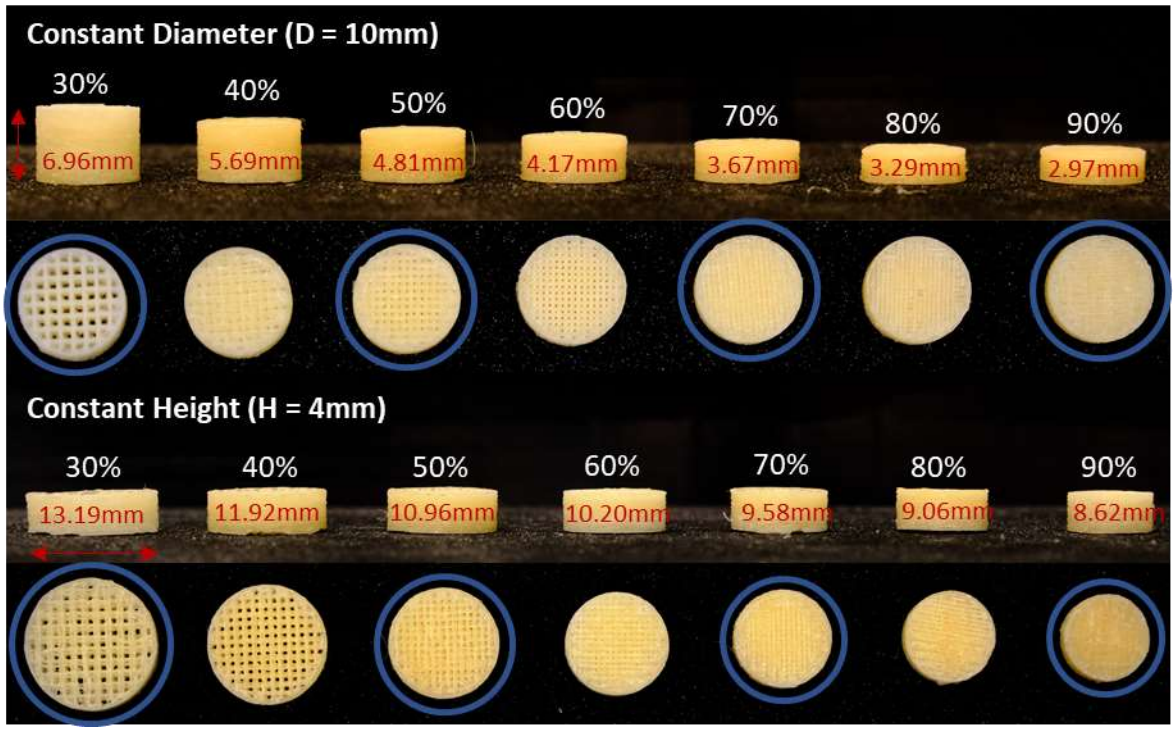

Figure 7. (Top) APF Eudragit-PAC tablets of constant weight and varying infill-density and height. (Bottom) APF Eudragit-PAC tablets of constant weight and varying infill-density and diameter. Tablet heights and diameters for each infill density are shown in red arrows. Blue circles indicate tablets taken forward for dissolution.

The Eudragit-PAC constant dose tablets (**Figure 7**) show good shape fidelity in comparison to the target dimensions, as seen in **Figure 8**. Deviation from average target diameter was greatest for the lowest infill tablets with a maximum deviation of 2.4% for the 30% infill CH tablets. Average tablet height deviation was minimal for both CH and CD designs with the majority of

prints within 1% of the target height. Average tablet weight was also very consistent both between geometries (CH and CD) and with varying infill density. All Eudragit-PAC CH and CD tablets (14 batches of 8 tablets each) conformed to comparable pharmacopeia weight uniformity specifications for batch produced tablets which require each dosage form to be within 85% - 115% of the average mass [31]. The 30%CH tablet showed the largest deviation at approximately 9% underweight. We suspect this was due to some material loss during tablet removal from the build plate which was more challenging for the more fragile lower infill designs. The thermal degradation temperature of the APF printed tablets were measured using TGA and no difference was observed between the onsets of the thermal degradation temperature for PAC and the printed tablets (data not shown). This applied to both Eudragit - PAC and Soluplus-PAC tablets. Drug content assays of printed material were measured at 100.3% ± 1.5 of the theoretical drug load (28.6% w/w) indicating no significant thermal degradation or change to API loading following granulation and printing. Coupled with the good weight uniformity of the printed tablets this suggests the simple constant dose geometry calculating method detailed in the methods section is suitable for controlling tablet dose using APF.

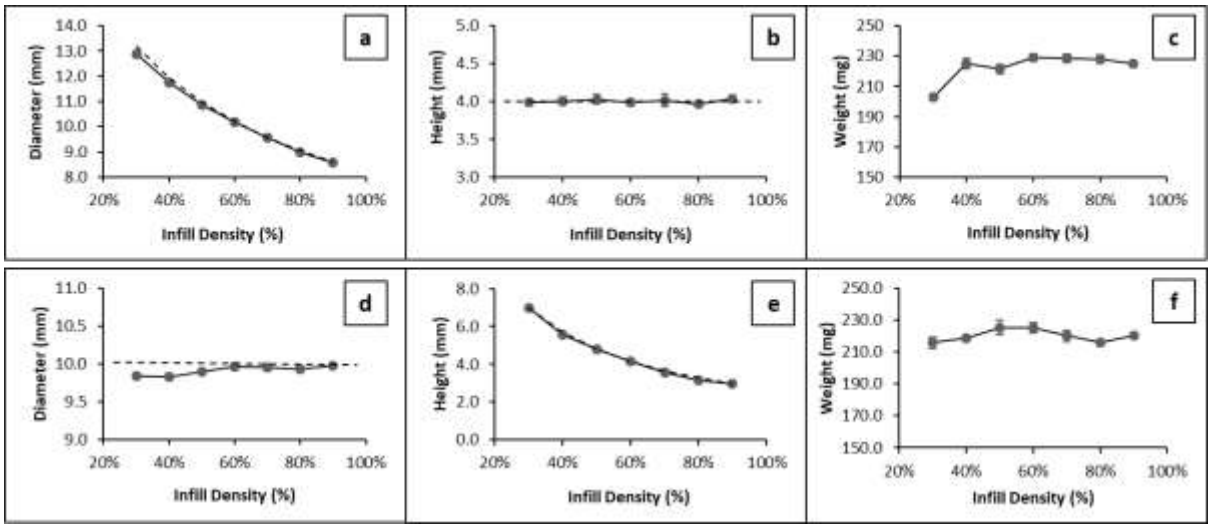

Figure 8. Dimensional and weight uniformity for CH (a-c) and CD (d-f) Eudragit-PAC tablets. The dash lines in (a), (b), (d) and (e) represent the target dimensions.

For Soluplus-PAC tablets (**Figure 9**), shape fidelity was comparable to the Eudragit-PAC prints with maximum average diameter deviations of 3% and maximum average height deviations of 2.3%, again occurring at the lowest infill density prints (**Figure 10**). The tablet weights showed excellent linear correlation with infill density indicated by a R^2 value of 0.996 and 0.997 for SM1 and SM2 tablets, respectively. For the different infill densities (n=6) all individual tablets were within 98-102% for SM1 and 95-104% for SM2 of the average weight at each infill density. The high accuracy and reproducibility of these tablets indicates the suitability of APF printing technique for pharmaceutical tablet manufacture where precise material deposition is required. Drug content assays of printed material were measured at $98.7\% \pm 3.7$ of the theoretical drug load (28.6% w/w) indicating no significant thermal degradation or change to API loading following granulation and printing.

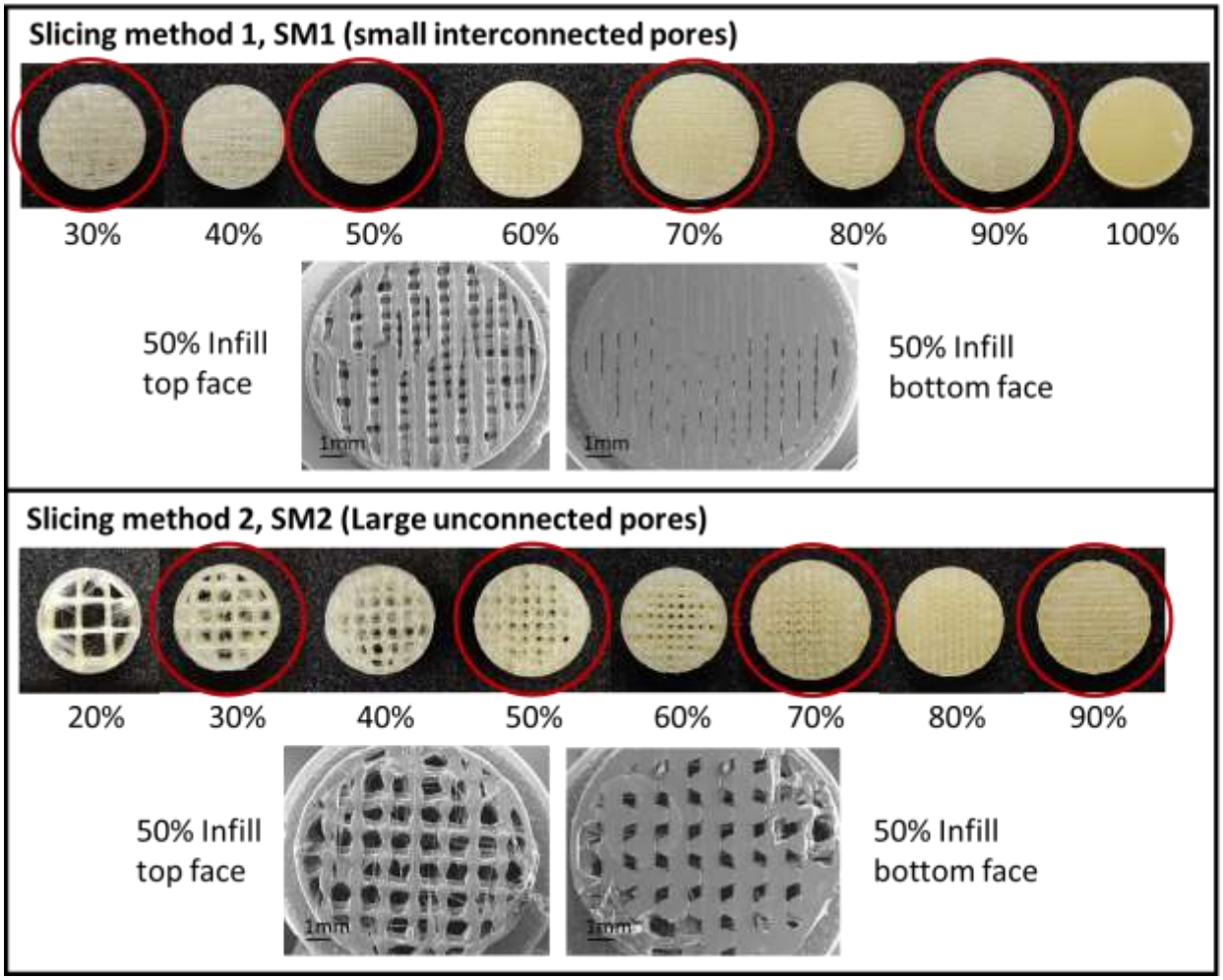

Figure 9. (Top) APF printed Soluplus-PAC tablets at 30% to 100% infill density printing using SM1 (Red circles indicate tablets carried forward for dissolution) with SEM image of top and bottom tablet face for 50% infill design. (Bottom) APF printed Soluplus-PAC tablets at 20% to 90% infill density printing using SM2 (Red circles indicate tablets carried forward for dissolution) with SEM image of top and bottom tablet face for 50% infill design.

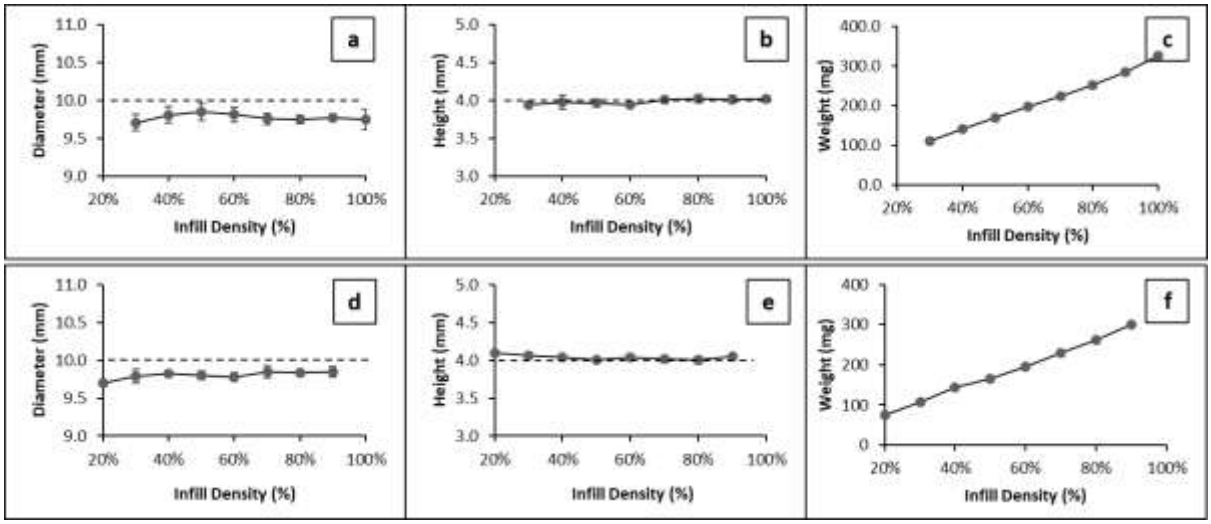

Figure 10. Dimensional and weight uniformity for Soluplus-PAC tablets with varying infill produced using SM1 (a-c) and SM2 (d-f). The dash lines represent target dimensions.

Effects of geometric scaling of tablet on *in vitro* drug release

Eudragit-PAC dissolution results are shown in **Figure 11a.** Cumulative release has been plotted for consistency but due to the constant dose between tablet designs this is also a close representation of the absolute drug release. With the exception of the 90%CH tablet all geometries reached at least 80% release within 30 minutes, satisfying pharmacopoeia requirements for immediate release solid dosage forms [32], indicating the suitability of Eudragit E for immediate release applications. Tablet geometric scaling, used to maintain drug dose between tablet designs whilst varying infill density, was not found to influence release profiles at 30%, 50% and 70% infill density. The well reported trend of decreasing release rate with increasing infill density (due to decreasing SA/V ratio) [11, 33] was seen to be almost identical between the CD and CH tablets. This finding can be explained by the very similar SA/V ratios between the CD and CH geometries (shown previously in **Table 4**) which is widely considered to have the greatest influence on geometry mediated drug release kinetics [34]. Interestingly, at the highest infill density studied, 90%, tablet geometry was seen to have a significant influence on the release profile which is highlighted by the large difference in mean

dissolution time (MDT) between the CD and CH geometries, shown in **Figure 11b**. The 90%CD tablets which had a thinner wider geometry had an average MDT of 9.3 minutes (50% release) compared to 24.1 minutes for the CH geometry.

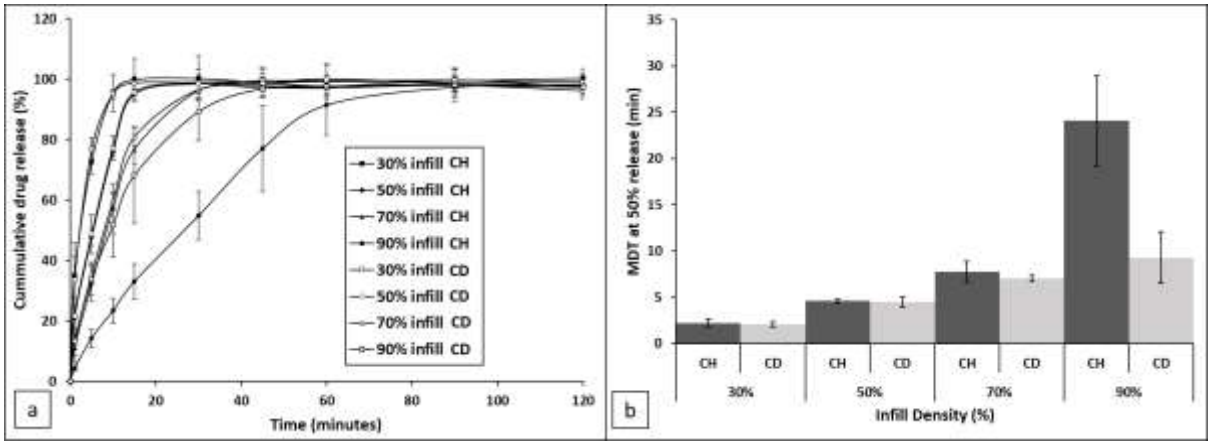

Figure 11. (a) *In vitro* drug release profiles of porous APF printed Eudragit-PAC tablets with either constant height (CH) or constant diameter (CD); (b) comparison of the mean dissolution time (MDT) of the tablets with infills between 30 to 90%.

To further understanding of how tablet diameter and height changes may impact the drug dissolution process and gain insight about the dissolution mechanism, spare tablets of the lowest (30%) and highest (90%) infill density were imaged periodically under USP 1 conditions (**Figure 12**). The low infill-density 30% Eudragit-PAC tablets showed no clear difference in dissolution time between the CD and CH geometry in agreement with the in vitro release data. Two clear dissolution steps were seen: erosion of the central porous region followed by erosion of the contour. At this low infill density, the large open pore structure is readily penetrated by dissolution media resulting in rapid erosion after approximately 3 minutes. The wall/contour region is comparatively "solid" with a significantly lower SA/V ratio compared to the central region and so is seen have a slower dissolution. In contrast at 90% infill a difference in both dissolution mechanism and dissolution rate between CD and CH geometries was seen. At 90% infill both geometries displayed a slower dissolution, dominated

by surface erosion mechanisms from the outside in, more similar to conventional nonporous tablets. Tablet diameter and thickness can be seen to gradually reduce as the erosion front penetrates the tablet until the tablet is completely dissolved. At this high infill density, slightly above the theoretical I_c (89%) the pore size is very small and merging between adjacent printpaths is likely, resulting in a pore geometry that cannot be readily penetrated by dissolution media. Thus, pore geometry is no longer open and interconnected and so the tablet behaves more as a solid. It has previously been shown that for surface eroding solid cylindrical tablets the ratio between tablet thickness and diameter ($R_{t/d}$) is important in determining release rate [7, 35, 36]. The closer the $R_{r/t}$ ratio to one, the more symmetrical the geometry is, such as a sphere or a cube. Therefore, the slower drug release in comparison to asymmetrical cylindrical geometry. For thin "slab" geometries with $R_{t/d}$ <1 cylinder thickness will go to zero before the diameter. The 90%CD tablet has a $R_{t/d}$ ratio of 0.3 compared to 0.47 for the 90%CH design. The lower $R_{t/d}$ for the CD design means it will maintain a relatively larger surface area during erosion giving it a faster release rate.

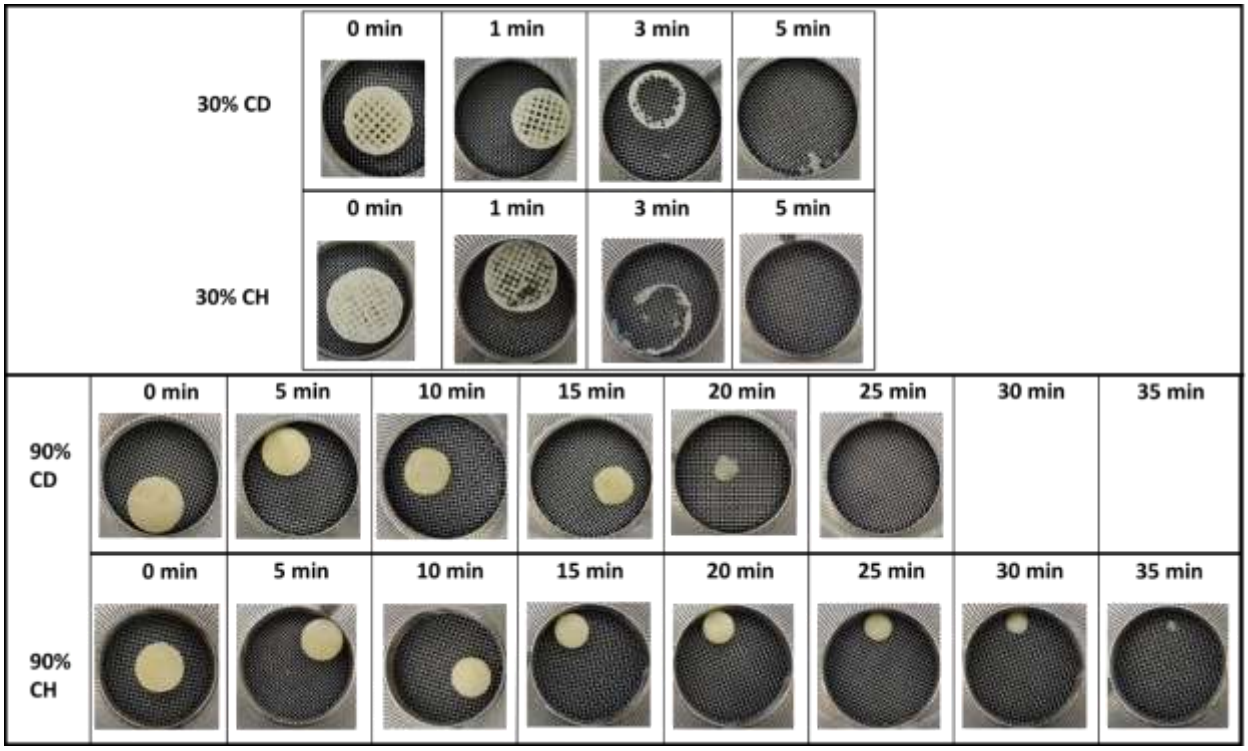

Figure 12. The effects of geometric scaling on the dissolution processes of 30% and 90% infill constant dose Eudragit-PAC tablets with either constant diameter (CD) or constant height (CH) (the images were taken at each time point during the in vitro drug release studies using USP 1 basket method).

A closer inspection of **Figure 12** shows that the 90%CD sample does not maintain its radial symmetry as would be expected for erosion of a monolithic cylinder as discussed above. It may be that the mechanical integrity of the print is not maintained, due to some penetration of dissolution media into the interior causing internal erosion, resulting in a rate of drug release more consistent with other degrees with lower percentage infills. In the case of the 90%CH sample, there is likely to be some penetration of the interior. However, due to the greater distance required to fully penetrate the interior (due to increased tablet height), the effect of internal erosion is much less leading to the overall rate of drug release being much slower. This finding highlights the importance of pore structure and tablet geometry in determining tablet dissolution and release mechanisms. SA/V ratio appears to drive dissolution behaviour for highly porous tablets that can be freely penetrated by dissolution media independent of tablet

geometry, whereas macro geometry and tablet $R_{t/d}$ control dissolution mechanics at high infill densities, such as 90%, where the tablet behaves more as a solid.

Effects of infill pattern on *in vitro* drug release

The Soluplus-PAC tablets were used to investigate the effects of infill pattern on *in vitro* drug release performance for swellable, erodible dosage forms. As seen in **Figure 13a**, the dissolution of the Soluplus-PAC tablets was much slower and more sustained than for the Eudragit-PAC formulation. At 50% infill density the dissolution took approximately 9 hours, increasing to several days for the 100% dense tablets. The decreased infill density can be seen to allow increased imbibition of dissolution media causing increased swelling and tablet dissolution.

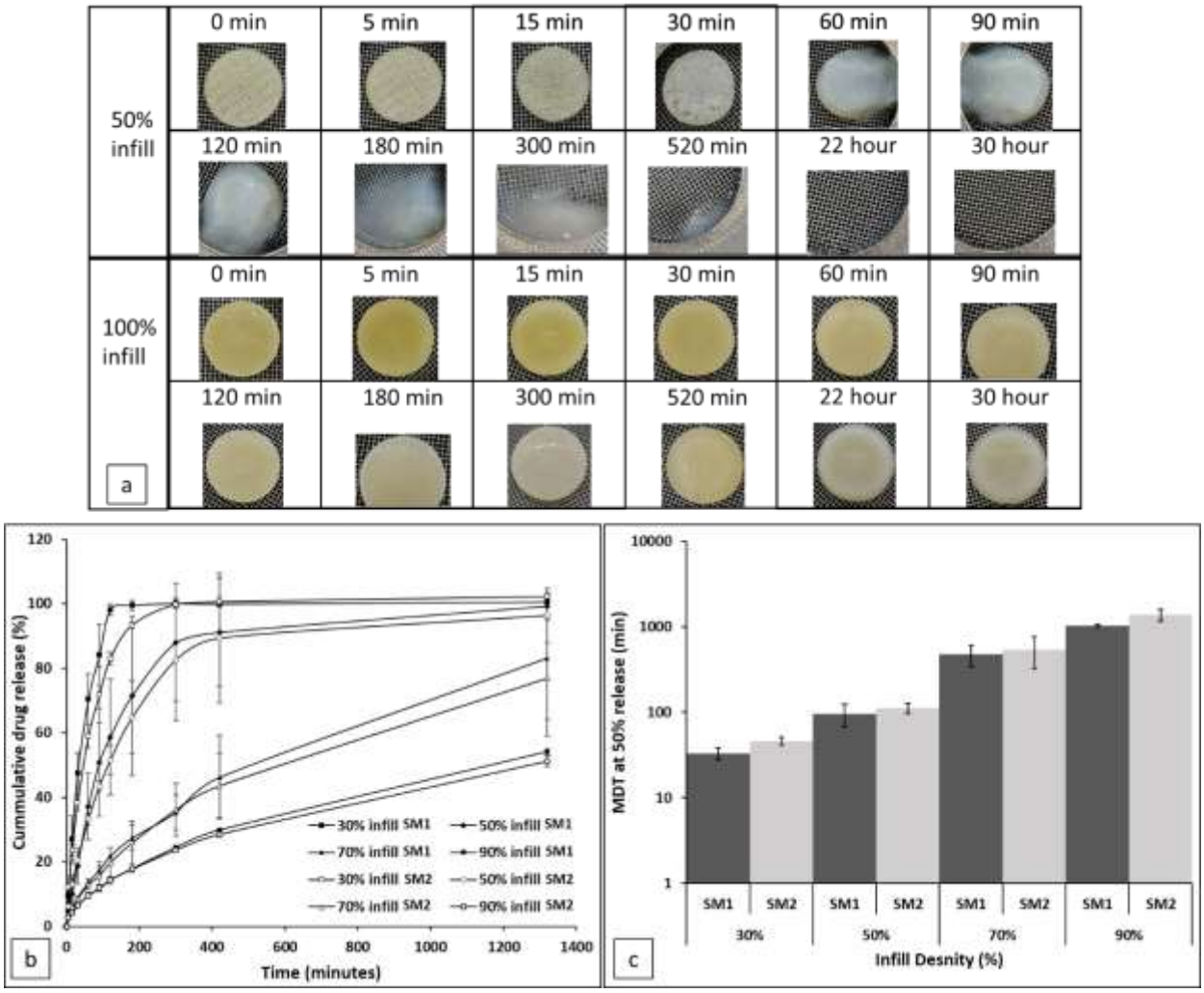

Figure 13. (a) Visual observation of the dissolution processes of Soluplus-PAC tablets (printed using SM1); (b) Paracetamol release profile from porous APF printed Soluplus-PAC tablets; (c) Mean dissolution time of the tablets to reach 50% cumulative release.

The release data shown for Soluplus-PAC is shown in **Figure 13b.** Despite the swellable properties of the polymer causing swelling and merging of the pore structure, infill density was still found to be a good release rate mediator for this formulation. The 30% SM1 design released quickest with 80% release within 90 minutes and the 90% infill designs released slowest reaching approximately 50% release at 22 hours. Lower infill density designs allowed increased dissolution media imbibition increasing the swelling and erosion of the polymer which increases the diffusion of the API [37]. The higher 70% and 90% infill designs approximate zero order release indicating Soluplus's potential for sustained release

applications. Interestingly the infill pattern used was not seen to significantly influence release results. Despite significantly different pore structure and SA/V ratio (shown previously in **Table 3**) there was no significant difference in release rate for the designs indicated by similar mean dissolution times (MDT) shown in **Figure 13c.** This finding would suggest that for swellable systems such as Soluplus it is simply the level of tablet porosity that mediates release rate and SA/V, and pore geometry is largely insignificant. This can be attributed to the pore geometry being largely lost as the pores became closed up during the significant swelling of printpaths.

Conclusion

This study assessed the suitability of APF for manufacturing non FDM printable formulations and investigated how tablet outer and inner geometry can be controlled using software to generate a wide range of release profiles independent of drug dose. Both Eudragit E and Soluplus were successfully printed without the need for additives. Constant dose printing of Eudragit-PAC tablets with varying geometry (tablet height or diameter) demonstrated that release performance was outer geometry independent for infill densities of 30-70% (i.e., tablet scaling can be effectively used to tune dose for porous tablets with minimal effect on release profile) but outer geometry dependant at 90% infill where the tablet behaves more as a solid. We suggest this is due to a fundamental pore structure change from open and interconnected to closed and disconnected which occurs at a critical infill density I_c. Below I_c release kinetics are driven by tablet SA/V and above I_c release kinetics are driven by tablet $R_{t/d}$. In contrast, release results on Soluplus-PAC tablets showed no dependence on SA/V ratio, indicating it is just the level of porosity, rather than pore structure that mediates drug release rate for highly swellable systems. These results give further insight into how formulation and hardware

independent parameters can be tuned to manufacture personalised pharmaceutical solid dosage forms at/close to the point of care.

Acknowledgement

We would like to thank the Enabling Innovation: Research to Application (EIRA), a Research England Connecting Capability Fund (CCF) project for providing the funding for the study. Additional thanks to Arburg for their Freeformer training and material qualification insight as well as PCE Automation for their technical support.

References:

[1] H. Öblom, J. Zhang, M. Pimparade, I. Speer, M. Preis, M. Repka, N. Sandler, 3D-printed isoniazid tablets for the treatment and prevention of tuberculosis—Personalized dosing and drug release, Aaps Pharmscitech, 20 (2019) 1-13.
[2] C. Curti, D.J. Kirby, C.A. Russell, Current formulation approaches in design and development of solid oral dosage forms through three-dimensional printing, Progress in Additive Manufacturing, 5 (2020) 111-123.
[3] S. Ayyoubi, J.R. Cerda, R. Fernández-García, P. Knief, A. Lalatsa, A.M. Healy, D.R. Serrano, 3D printed spherical mini-tablets: Geometry versus composition effects in controlling dissolution from personalised solid dosage forms, International Journal of Pharmaceutics, 597 (2021) 120336.
[4] T. McDonagh, P. Belton, S. Qi, Direct Granule Feeding of Thermal Droplet Deposition 3D Printing of Porous Pharmaceutical Solid Dosage Forms Free of Plasticisers, Pharm Res, (2022).
[5] B. Zhang, A. Gleadall, P. Belton, T. McDonagh, R. Bibb, S. Qi, New insights into the effects of porosity, pore length, pore shape and pore alignment on drug release from extrusionbased additive manufactured pharmaceuticals, Additive Manufacturing, 46 (2021) 102196.
[6] J. Siepmann, K. Podual, M. Sriwongjanya, N.A. Peppas, R. Bodmeier, A new model describing the swelling and drug release kinetics from hydroxypropyl methylcellulose tablets, Journal of pharmaceutical sciences, 88 (1999) 65-72.
[7] I. Katzhendler, A. Hoffman, A. Goldberger, M. Friedman, Modeling of Drug Release from Erodible Tablets, Journal of Pharmaceutical Sciences, 86 (1997) 110-115.
[8] A. Goyanes, P. Robles Martinez, A. Buanz, A.W. Basit, S. Gaisford, Effect of geometry on drug release from 3D printed tablets, International Journal of Pharmaceutics, 494 (2015) 657-663.
[9] M.V.S. Varma, A.M. Kaushal, A. Garg, S. Garg, Factors affecting mechanism and kinetics of drug release from matrix-based oral controlled drug delivery systems, American Journal of drug delivery, 2 (2004) 43-57.
[10] M.P. Paarakh, P.A. Jose, C.M. Setty, G.V. Peter, Release kinetics–concepts and applications, Int J Pharm Res Technol, 8 (2018) 12-20.

[11] H. Kadry, T.A. Al-Hilal, A. Keshavarz, F. Alam, C. Xu, A. Joy, F. Ahsan, Multi-purposable filaments of HPMC for 3D printing of medications with tailored drug release and timed-absorption, International journal of pharmaceutics, 544 (2018) 285-296.
[12] J. Zhang, W. Yang, A.Q. Vo, X. Feng, X. Ye, D.W. Kim, M.A. Repka, Hydroxypropyl methylcellulose-based controlled release dosage by melt extrusion and 3D printing: Structure and drug release correlation, Carbohydrate polymers, 177 (2017) 49-57.
[13] M. Sadia, A. Sośnicka, B. Arafat, A. Isreb, W. Ahmed, A. Kelarakis, M.A. Alhnan, Adaptation of pharmaceutical excipients to FDM 3D printing for the fabrication of patient-tailored immediate release tablets, International journal of pharmaceutics, 513 (2016) 659-668.
[14] Y. Yang, H. Wang, X. Xu, G. Yang, Strategies and mechanisms to improve the printability of pharmaceutical polymers Eudragit® EPO and Soluplus®, International Journal of Pharmaceutics, 599 (2021) 120410.
[15] K.A. Khan, The concept of dissolution efficiency, Journal of pharmacy and pharmacology, 27 (1975) 48-49.
[16] W. Kaialy, H. Bello, K. Asare-Addo, A. Nokhodchi, Effect of solvent on retarding the release of diltiazem HCl from Polyox-based liquisolid tablets, Journal of Pharmacy and Pharmacology, 68 (2016) 1396-1402.
[17] E.I. Nep, M.H. Mahdi, A.O. Adebisi, C. Dawson, K. Walton, P.J. Bills, B.R. Conway, A.M. Smith, K. Asare-Addo, The influence of hydroalcoholic media on the performance of Grewia polysaccharide in sustained release tablets, International journal of pharmaceutics, 532 (2017) 352-364.
[18] T.D. Reynolds, S.A. Mitchell, K.M. Balwinski, Investigation of the effect of tablet surface area/volume on drug release from hydroxypropylmethylcellulose controlled-release matrix tablets, Drug development and industrial pharmacy, 28 (2002) 457-466.
[19] M. Kyobula, A. Adedeji, M.R. Alexander, E. Saleh, R. Wildman, I. Ashcroft, P.R. Gellert, C.J. Roberts, 3D inkjet printing of tablets exploiting bespoke complex geometries for controlled and tuneable drug release, Journal of Controlled Release, 261 (2017) 207-215.
[20] B.K. Lee, Y.H. Yun, J.S. Choi, Y.C. Choi, J.D. Kim, Y.W. Cho, Fabrication of drug-loaded polymer microparticles with arbitrary geometries using a piezoelectric inkjet printing system, International Journal of Pharmaceutics, 427 (2012) 305-310.
[21] D. Markl, J.A. Zeitler, A Review of Disintegration Mechanisms and Measurement Techniques, Pharm Res, 34 (2017) 890-917.
[22] P. Sriamornsak, N. Thirawong, K. Korkerd, Swelling, erosion and release behavior of alginate-based matrix tablets, European Journal of Pharmaceutics and Biopharmaceutics, 66 (2007) 435-450.
[23] K. Shi, J.P. Salvage, M. Maniruzzaman, A. Nokhodchi, Role of release modifiers to modulate drug release from fused deposition modelling (FDM) 3D printed tablets, International Journal of Pharmaceutics, 597 (2021) 120315.
[24] B. Wittbrodt, J.M. Pearce, The effects of PLA color on material properties of 3-D printed components, Additive Manufacturing, 8 (2015) 110-116.
[25] R.N. Shamma, M. Basha, Soluplus®: A novel polymeric solubilizer for optimization of Carvedilol solid dispersions: Formulation design and effect of method of preparation, Powder Technology, 237 (2013) 406-414.
[26] Y. Nguyen Thi, K. Rademann, F. Emmerling, Direct evidence of polyamorphism in paracetamol, CrystEngComm, 17 (2015) 9029-9036.
[27] M. Zhao, S.A. Barker, P.S. Belton, C. McGregor, D.Q.M. Craig, Development of fully amorphous dispersions of a low Tg drug via co-spray drying with hydrophilic polymers, European Journal of Pharmaceutics and Biopharmaceutics, 82 (2012) 572-579.

[28] S. Qi, A. Gryczke, P. Belton, D.Q.M. Craig, Characterisation of solid dispersions of paracetamol and EUDRAGIT® E prepared by hot-melt extrusion using thermal, microthermal and spectroscopic analysis, International Journal of Pharmaceutics, 354 (2008) 158-167.
[29] T. Parikh, S.S. Gupta, A. Meena, A.T.M. Serajuddin, Investigation of thermal and viscoelastic properties of polymers relevant to hot melt extrusion, III: polymethacrylates and polymethacrylic acid based polymers, Journal of Excipients and Food Chemicals; Vol 5 No 1 (2014), (2014).
[30] H. Lim, S.W. Hoag, Plasticizer Effects on Physical–Mechanical Properties of Solvent Cast Soluplus® Films, AAPS PharmSciTech, 14 (2013) 903-910.
[31] Uniformity of Dosage Units, in, United States Pharmacopeial Convention, 2011.
[32] Recommendations on methods for dosage forms testing, in, European Pharmacopoeia 8.0 5.17.1, 2010.
[33] N.A. Elkasabgy, A.A. Mahmoud, A. Maged, 3D printing: An appealing route for customized drug delivery systems, International Journal of Pharmaceutics, 588 (2020) 119732.
[34] P.R. Martinez, A. Goyanes, A.W. Basit, S. Gaisford, Influence of Geometry on the Drug Release Profiles of Stereolithographic (SLA) 3D-Printed Tablets, AAPS PharmSciTech, 19 (2018) 3355-3361.
[35] H.B. Hopfenberg, Controlled Release from Erodible Slabs, Cylinders, and Spheres, in: Controlled Release Polymeric Formulations, AMERICAN CHEMICAL SOCIETY, 1976, pp. 26-32.
[36] D.O. Cooney, Effect of geometry on the dissolution of pharmaceutical tablets and other solids: Surface detachment kinetics controlling, AIChE Journal, 18 (1972) 446-449.
[37] J. Siepmann, N.A. Peppas, Modeling of drug release from delivery systems based on hydroxypropyl methylcellulose (HPMC), Advanced drug delivery reviews, 64 (2012) 163-174.